

# Isomorphous Co<sup>II</sup> and Mn<sup>II</sup> materials of tetrazolate-5-carboxylate with an unprecedented self-penetrating net and distinct magnetic behaviours†

Qin-Xiang Jia,<sup>a</sup> Yan-Qin Wang,<sup>a</sup> Qi Yue,<sup>a</sup> Qing-Lun Wang<sup>b</sup> and En-Qing Gao<sup>\*a</sup>

Received (in Cambridge, UK) 11th July 2008, Accepted 5th August 2008

First published as an Advance Article on the web 22nd September 2008

DOI: 10.1039/b811865e

**Two isomorphous Co<sup>II</sup> and Mn<sup>II</sup> three-dimensional coordination polymers with tetrazolate-5-carboxylate as magnetic mediator exhibit an unprecedented 3,4-connected self-penetrating net topology; a combination of canted antiferromagnetism and metamagnetism was observed in the Co<sup>II</sup> compound, whereas the Mn<sup>II</sup> compound shows typical antiferromagnetic behaviors.**

The design and synthesis of molecular magnetic materials have attracted considerable attention in recent years.<sup>1</sup> The great diversity and versatility of coordination and supramolecular chemistry have provided great opportunities to discover new magnetic materials and to better understand fundamental magnetic phenomena, such as spin canting and metamagnetism.<sup>2</sup> One of the most important factors influencing the magnetic behaviors is the nature of the bridge between paramagnetic centers, which governs the nearest-neighboring magnetic coupling. Up to now, only several types of multiatomic bridging ligands that mediate strong magnetic coupling have been investigated, such as pseudohalides (cyanide, azide, dicyanamide), carboxylates, oxalate, cyclic diazines, *etc.*<sup>3,4</sup> There is always great interest in searching for new bridging ligands.<sup>5</sup> Recently, some efforts have been devoted to tetrazole derivatives,<sup>5c-f</sup> which have a rich coordination chemistry. We are interested in tetrazolate-5-carboxylate (tzc), which is the simplest ligand that contains both tetrazolate and carboxylate but has not yet been explored in coordination chemistry. The ligand is expected to be a versatile bridge that can mediate strong magnetic coupling. In this paper, we report the first two coordination compounds with this ligand, [M<sub>2</sub>(tzc)<sub>2</sub>(bpea)] (M = Co<sup>II</sup>, **1**, and Mn<sup>II</sup>, **2**; bpea = 1,2-bis(4-pyridyl)ethane), in which two-dimensional (2D) layers with μ<sub>3</sub>-tzc bridges are pillared by the bpea spacers to generate a three-dimensional (3D) structure with unprecedented 3,4-connected self-penetrating topology. The isomorphism of the two compounds allows us to investigate the exclusive influence of magnetic anisotropy on bulk magnetic behaviors: the Co<sup>II</sup> compound shows a combination of canted antiferromagnetism and metamagnetism, whereas the Mn<sup>II</sup> compound is a typical antiferromagnetic system.

The compounds were prepared by the hydrothermal reactions of sodium ethyl tetrazolate-5-carboxylate, M(OAc)<sub>2</sub>·4H<sub>2</sub>O and bpea.† X-ray analysis‡ revealed that the two

compounds are isomorphous and that the structure consists of neutral 2D M(II)-tzc layers interlinked by the bpea spacers. The metal ion is chelated by two tzc ligands through tetrazole nitrogens and carboxylate oxygens, and a distorted octahedral geometry is completed by two nitrogen atoms from a third tzc ligand and a bpea ligand (Fig. 1). Two nitrogen atoms (N3A and N4) and two oxygen atoms (O1, O2B) from three tzc ligands define an equatorial quasi-plane, and the axial positions are occupied by a tetrazole nitrogen (N1B) and a pyridyl nitrogen (N5). The M–N/O distances in **1** (2.10–2.27 Å) are about 0.1 Å shorter than those in **2** (2.18–2.34 Å). The tzc ligand exhibits a μ<sub>3</sub> pentadentate bridging mode with all nitrogen atoms and oxygen atoms except for N2 being involved in coordination, and it constitutes three types of bridges between metal ions: (i) the bischelating O<sub>2</sub>C<sub>2</sub>N<sub>2</sub> bridge resembling oxalate, with M···M = 5.53 Å (**1**) and 5.74 Å (**2**); (ii) the double N–N bridge from two tetrazole rings, which generates a centrosymmetric quasi-planar M(N–N)<sub>2</sub>M hexagon with M···M = 4.35 (**1**) and 4.54 Å (**2**); (iii) the 1,3-tetrazole bridge with M···M = 6.45 (**1**) and 6.65 Å (**2**). Such a coordination mode of the tzc ligand leads to a two-dimensional undulated layer parallel to the *bc* plane (Fig. 2(a)). As depicted in Fig. 2(b), viewing both the metal ion and the tzc ligand as three-connecting nodes, the topology of the 2D net is 4-8.<sup>2</sup> From magnetic points of view, it is worth noting that neighboring metal coordination polyhedra connected by the non-centrosymmetric 1,3-tetrazole or O<sub>2</sub>C<sub>2</sub>N<sub>2</sub> bridges are slanted to each other, with the dihedral angles between the neighboring equatorial planes being 77° in **1** and 79° in **2**.

The ditopic bpea ligand binds two metal ions from neighboring layers, and hence the 2D layers are pillared into a 3D framework. Pillared frameworks have attracted special

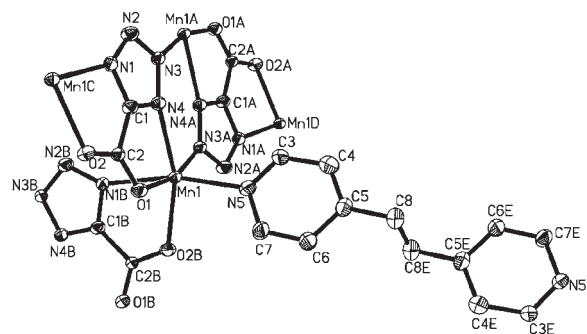
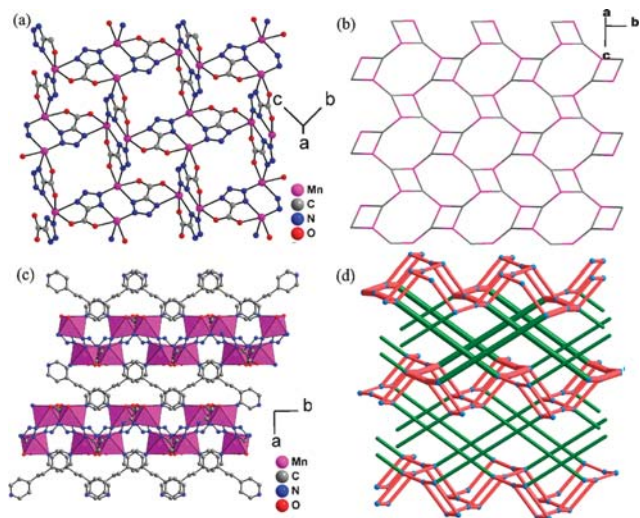


Fig. 1 The coordination environment in **2**. Displacement ellipsoids are drawn at the 30% probability level.

<sup>a</sup> Shanghai Key Laboratory of Green Chemistry and Chemical Processes, Department of Chemistry, East China Normal University, Shanghai, 200062, China. E-mail: eqgao@chem.ecnu.edu.cn

<sup>b</sup> Department of Chemistry, Nankai University, Tianjin, 300071, China † CCDC 694330 and 694331. For crystallographic data in CIF or other electronic format see DOI: 10.1039/b811865e



**Fig. 2** The extended structure of **2**. (a) A 2D layer with tzc as  $\mu_3$ -bridging ligands, (b) the 2D topology, (c) the 3D structure, and (d) the 3D topology with self-catenation highlighted by bold lines.

attention in the pursuit of molecular magnetic materials.<sup>6</sup> To adapt to the relatively slanted coordination polyhedra in the layers, the pillars between the layers are also systematically slanted in two different directions. As a result, the shortest interlayer  $M \cdots M$  distance (8.04 Å in **1** and 7.94 Å in **2**), is much shorter than those spanned by the pillar (13.42 Å in **1** and 13.63 Å in **2**). Taking into account the bpea linkers, the metal ions become 4-connecting nodes, and consequently, with tzc still as 3-connecting nodes, the 3D network can be viewed as a 3,4-connected binodal net (Fig. 2(d)) based on 2D ( $4 \cdot 8^2$ ) nets. The Schläfli notation is  $(4 \cdot 8^2 \times 10^3)(4 \cdot 8^2)$ . To our knowledge, such a net has not been elucidated.<sup>7</sup> It is worth noting that the net is a new example of the rare self-penetrating 3D networks:<sup>8</sup> each 10-membered shortest circuit across the interlayer space is catenated by two other 10-membered circuits (3-fold catenation). This is interesting because self-penetration usually occurs with 2-fold catenation.<sup>7</sup> The complicated catenation reported here results from the presence of two mutually slanted sets of long bpea pillars in the interlayer space.

The magnetic susceptibilities of **1** and **2** were measured in the 2–300 K temperature range under 1 kOe and are shown as  $\chi T$  vs.  $T$  plots in Fig. 3(a). The  $\chi T$  value ( $3.25 \text{ emu K mol}^{-1}$ ) per Co(II) at 300 K is typical of octahedral Co(II) with an unquenched orbital momentum. The product first decreases smoothly to a minimum of 0.99 at 16 K, then rises rapidly to a

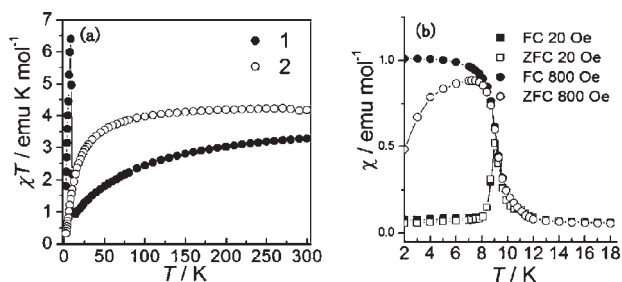


**Fig. 3** (a) Thermal variation of  $\chi T$  of **1** and **2** at 1 kOe; (b) ZFC and FC  $\chi(T)$  curves of **1** at different fields.

sharp maximum of  $6.40 \text{ emu K mol}^{-1}$  at 8 K, and finally drops rapidly due to saturation effects. The  $1/\chi$  vs.  $T$  data above 45 K follows the Curie–Weiss law with  $C = 3.96 \text{ emu mol}^{-1} \text{ K}$  and  $\theta = -61.6 \text{ K}$ . The negative value of  $\theta$  and the initial decrease of  $\chi T$  should be due to the concurrent effects of spin–orbital coupling of Co(II) and the antiferromagnetic coupling through the  $\mu_3$ -tzc bridge. The steep rises in  $\chi T$  at low temperature indicate the onset of a ferromagnetic-like correlation. This phenomenon is attributable to spin canting, well consistent with the systematic alternation of the slanted metal polyhedra throughout the layer: the antiferromagnetically coupled adjacent spins within the layers are not perfectly antiparallel but canted to each other, and the resulting uncompensated moments correlate in a ferromagnetic-like fashion and develop into long-range ordering. The weak ferromagnetism has been confirmed by the FC (field cooled) and ZFC (zero-field cooled) magnetization measurements under different fields (Fig. 3(b), in the form of  $\chi(T)$  curves). The ZFC and FC curves at 20 Oe exhibit only very small differences and both have a sharp maximum at *ca.* 9 K, suggesting the occurrence of interlayer antiferromagnetic ordering below  $T_N = 9 \text{ K}$ . However, at a higher field of 800 Oe, the ZFC and FC curves diverge below 9 K, with the ZFC maximum shifted to lower temperature and the FC maximum not observed. The FC magnetization rises rapidly below *ca.* 10 K and approaches saturation below 7 K, indicating the onset of spontaneous magnetization. The behaviors suggest that the interlayer antiferromagnetic ordering is broken by the higher field to generate a weak ferromagnetic state, typical of metamagnetism.

Further information comes from the isothermal magnetization measurements (Fig. 4). The features that the magnetization increases slowly with the field above 10 kOe and that the value of  $0.59 N\beta$  at 50 kOe is far from saturation are consistent with the antiferromagnetic nature of the interaction between neighboring metal ions. The saturation magnetization ( $M_s$ ) for a pseudo-octahedral Co(II) ion at very low temperature ( $< 20 \text{ K}$ ) is usually  $2.1\text{--}2.5 N\beta$  with  $S_{\text{eff}} = 1/2$  and  $g_{\text{eff}} = 4.1\text{--}5.0$ .<sup>9</sup> Extrapolating the high-field linear part of the magnetization curve to zero field gives a value of  $0.17 N\beta$ , which may be taken as the weak magnetization ( $M_w$ ) arising

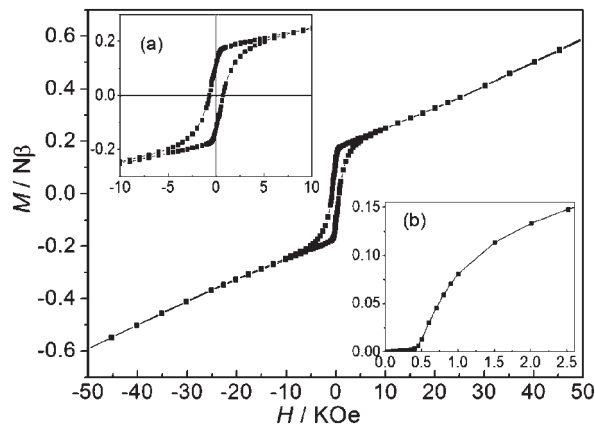


**Fig. 4** Isothermal magnetization of **1** at 2 K. Insets: the blow-up of the hysteresis loop (a) and initial magnetization curve (b) under lower fields.

from spin canting. Accordingly, the canting angle can be estimated to be in the range of 3.9–4.6°. The sigmoidal shape of the initial  $M(H)$  curve at low field (Fig. 4, inset b) confirms the field-induced metamagnetism, with a critical field of 0.6 kOe (2 K), at which the  $\partial M/\partial H$  curve exhibits a maximum. The hysteresis loop at 2 K shows a remnant magnetization of 0.13  $N\beta$  and a coercive field of 0.7 kOe (Fig. 4, inset a).

The  $\chi T$  value of **2** at 300 K is 4.18 emu mol<sup>-1</sup> K, slightly lower than the spin-only value of 4.37 emu mol<sup>-1</sup> K for  $S = 5/2$ . The product decreases monotonically upon cooling, and the  $1/\chi$  vs.  $T$  data above 40 K follow the Curie–Weiss law with  $C = 4.38$  emu mol<sup>-1</sup> K and  $\theta = -10.5$  K. Such behaviors reveal antiferromagnetic coupling between Mn(II) ions.

It is interesting to note that **2** shows no indications of spin canting, which has been evidenced for the isomorphous Co(II) species (**1**). As well established, spin canting can arise from two mechanisms:<sup>10</sup> (i) single-ion anisotropy, which energetically favors spin canting if the anisotropy axes on neighboring sites are different; (ii) the antisymmetric Dzyaloshinsky–Moriya (DM) interaction, which tends to align the interacting spins in a perpendicular way and requires  $g$ -factor anisotropy. It is well known that pseudo-octahedral Co(II) has strong magnetic anisotropy resulting from unquenched orbital momentum and first-order spin–orbit coupling. Therefore, both mechanisms favor the spin canting in **1**. On the other hand, since Mn(II) usually has negligible  $g$ -factor anisotropy due to the <sup>6</sup>A ground state, the DM interaction is too weak to cause canting and the canting in Mn(II) compounds are usually attributed to single-ion anisotropy of Mn(II),<sup>2</sup> which is due to zero-field splitting and sensitive to geometrical distortion. It is likely that the zero-field splitting in **2** is too small to cause observable canting.

In conclusion, we have described two new metal-organic magnetic materials with tzc as the bridges mediating magnetic coupling and with bpea as the pillars interlinking M(II)-tzc layers. The materials exhibit an unprecedented 3,4-connected self-penetrating net. Although isomorphous, the two materials show remarkable differences in magnetism: the Co(II) material combines canted antiferromagnetism and metamagnetism due to the strong anisotropy, while the Mn(II) one shows usual antiferromagnetic behaviors.

We are thankful for NSFC (20571026 and 20771038), MOE (NCET-05-0425), Shanghai Leading Academic Discipline Project (B409), and STCSM (06SR07101) for financial support.

## Notes and references

† *Synthesis*: The reaction of Co(OAc)<sub>2</sub>·4H<sub>2</sub>O (0.05 mmol, 0.012 g), sodium ethyl tetrazolate-5-carboxylate (0.05 mmol, 0.008 g), and 1,2-bis(4-pyridyl)ethane (0.025 mmol, 0.005 g) in H<sub>2</sub>O (8 mL) at 110 °C over 5 days yielded red prism crystals of **1**. Yield, 60.8%. **2** was synthesized by a similar procedure. Yield, 19.3%. Anal. Calc. for C<sub>8</sub>H<sub>6</sub>CoN<sub>5</sub>O<sub>2</sub> (**1**): C, 36.52; H, 2.30; N, 26.62. Found: C, 36.66; H,

2.58; N, 27.06%. Main IR bands (KBr, cm<sup>-1</sup>): 1646s, 1617m, 1509m, 1458s, 1345s, 831m, 546m. Anal. calcd. for C<sub>8</sub>H<sub>6</sub>MnN<sub>5</sub>O<sub>2</sub> (**2**): C, 37.08; H, 2.33; N, 27.03. Found: C, 37.49; H, 2.65; N, 27.28%. Main IR bands (KBr, cm<sup>-1</sup>): 1650s, 1612s, 1506s, 1435s, 1340s, 837s, 546s. § *Crystal data*: **1**, C<sub>8</sub>H<sub>6</sub>CoN<sub>5</sub>O<sub>2</sub>,  $M_r = 263.11$ , monoclinic, space group  $P2_1/c$ ,  $a = 11.604(9)$ ,  $b = 9.302(7)$ ,  $c = 9.161(7)$  Å,  $\beta = 98.626(13)^\circ$ ,  $V = 977.6(13)$  Å<sup>3</sup>,  $Z = 4$ ,  $\mu(\text{Mo-K}\alpha) = 1.747$  mm<sup>-1</sup>,  $\lambda = 0.71073$  Å,  $D_c = 1.788$  g cm<sup>-3</sup>,  $T = 293(2)$  K,  $S = 1.025$ ,  $R1 = 0.0406$  for 1420 reflections with  $I > 2\sigma(I)$ , and  $wR2 = 0.0854$  for 1925 independent reflections ( $R_{\text{int}} = 0.0337$ ). **2**, C<sub>8</sub>H<sub>6</sub>MnN<sub>5</sub>O<sub>2</sub>,  $M_r = 259.12$ , monoclinic, space group  $P2_1/c$ ,  $a = 11.833(2)$ ,  $b = 9.7295(17)$ ,  $c = 9.2017(16)$  Å,  $\beta = 101.990(2)^\circ$ ,  $V = 1036.2(3)$  Å<sup>3</sup>,  $Z = 4$ ,  $\mu(\text{Mo-K}\alpha) = 1.266$  mm<sup>-1</sup>,  $\lambda = 0.71073$  Å,  $D_c = 1.661$  g cm<sup>-3</sup>,  $T = 298(2)$  K,  $S = 0.921$ ,  $R1 = 0.0585$  for 1174 reflections with  $I > 2\sigma(I)$ , and  $wR2 = 0.1718$  for 1956 independent reflections ( $R_{\text{int}} = 0.0374$ ).

- (a) J. S. Miller and M. Drillon, *Magnetism: Molecules to Materials I-V*, Wiley-VCH, Weinheim, 2001–2005; (b) D. Gatteschi and R. Sessoli, *Angew. Chem., Int. Ed.*, 2003, **42**, 268; (c) C. Coulon, H. Miyasaka and R. Clérac, *Struct. Bonding*, 2006, **122**, 163.
- R. L. Carlin, *Magnetochemistry*, Springer, Berlin-Heidelberg, 1986.
- (a) M. Ohba and H. Okawa, *Coord. Chem. Rev.*, 2000, **198**, 313; (b) J. Cernak, M. Orendac, I. Potocnak, J. Chomic, A. Orendacova, J. Skorsepa and A. Feher, *Coord. Chem. Rev.*, 2002, **224**, 51; (c) J. Ribas, A. Escuer, M. Monfort, R. Vicente, R. Cortes, L. Lezama and T. Rojo, *Coord. Chem. Rev.*, 1999, **195**, 1027; (d) X.-Y. Wang, Z.-M. Wang and S. Gao, *Chem. Commun.*, 2008, 281; (e) S. R. Batten and K. S. Murray, *Coord. Chem. Rev.*, 2003, **246**, 103.
- (a) S. C. Manna, E. Zangrando, M. G. B. Drew, J. Ribas and N. R. Chaudhuri, *Eur. J. Inorg. Chem.*, 2006, 481; (b) J. A. Real, A. B. Gaspar, V. Niel and M. C. Munoz, *Coord. Chem. Rev.*, 2003, **236**, 121; (c) G. Peobide, W.-G. Wang, O. Castillo, A. Luque, P. Roman, G. Tagliabue, S. Galli and J. A. R. Navarro, *Inorg. Chem.*, 2008, **47**, 5267.
- (a) J.-R. Li, Q. Yu, Y. Tao, X.-H. Bu, J. Ribas and S. R. Batten, *Chem. Commun.*, 2007, 2290; (b) A. Rodriguez-Dieguez, J. Cano, R. Kivekas, A. Debdoubi and E. Colacio, *Inorg. Chem.*, 2007, **46**, 2503; (c) E.-Q. Gao, N. Liu, A.-L. Cheng and S. Gao, *Chem. Commun.*, 2007, 2470; (d) J.-Y. Zhang, Y. Ma, A.-L. Cheng, Q. Yue, Q. Sun and E.-Q. Gao, *Dalton Trans.*, 2008, 2061; (e) A. Rodriguez, R. Kivekas and E. Colacio, *Chem. Commun.*, 2005, 5228; (f) N. Liu, Q. Yue, Y.-Q. Wang, A.-L. Cheng and E.-Q. Gao, *Dalton Trans.*, 2008, 4621.
- (a) P.-P. Liu, A.-L. Cheng, N. Liu, W.-W. Sun and E. Q. Gao, *Chem. Mater.*, 2007, **19**, 2724; (b) X.-Y. Wang, L. Wang, Z.-M. Wang and S. Gao, *J. Am. Chem. Soc.*, 2006, **128**, 674; (c) M. Kurmoo and H. Kumagai, *Mol. Cryst. Liq. Cryst.*, 2002, **376**, 555.
- (a) *Reticular Chemistry Structure Resource (RCSR)*, <http://rcsr.anu.edu.au/>; (b) *Euclidean Patterns in Non-Euclidean Tilings (EPINET)*, <http://epinet.anu.edu.au/>; (c) V. A. Blatov and A. P. Shevchenko, *TOPOS 4.0*, Samara State University, Russia.
- (a) L. Carlucci, G. Ciani and D. M. Proserpio, *Coord. Chem. Rev.*, 2003, **246**, 247; (b) X.-L. Wang, C. Qin, E.-B. Wang, Z.-M. Su, L. Xu and S. R. Batten, *Chem. Commun.*, 2005, 4789.
- (a) A. Rujiwatra, C. J. Kepert, J. B. Claridge, M. J. Rosseinsky, H. Kumagai and M. Kurmoo, *J. Am. Chem. Soc.*, 2001, **123**, 10584; (b) H. Jankovics, M. Daskalakis, C. P. Raptopoulou, A. Terzis, V. Tangoulis, J. Giapintzakis, T. Kiss and A. Salifoglou, *Inorg. Chem.*, 2002, **41**, 3366; (c) P. Yin, S. Gao, L.-M. Zheng, Z.-M. Wang and X.-Q. Xin, *Chem. Commun.*, 2003, 1076; (d) W.-K. Chang, R. K. Chiang, Y.-C. Jiang, S.-L. Wang, S. F. Lee and K. H. Lii, *Inorg. Chem.*, 2004, **43**, 2564.
- (a) I. Dzyaloshinsky, *J. Phys. Chem. Solids*, 1958, **4**, 241; (b) T. Moriya, *Phys. Rev.*, 1960, **120**, 91; (c) T. Moriya, *Phys. Rev.*, 1960, **117**, 635.